ELSEVIER

Contents lists available at ScienceDirect

Materialia

journal homepage: www.elsevier.com/locate/mtla



A catalogue of metallic glass-forming alloy systems

Weijie Xie ^{a,b,#}, Mingxing Li ^{a,#}, Yitao Sun ^{a,#,*}, Chao Wang ^a, Liwei Hu ^a, Yanhui Liu ^{a,c,*}

- ^a Institute of Physics, Chinese Academy of Sciences, 100190 Beijing, China
- ^b School of Physics, University of Chinese Academy of Sciences, Beijing 100049, China
- ^c Center of Materials Science and Optoelectronics Engineering, University of Chinese Academy of Sciences, Beijing 100049, China

ARTICLE INFO

Keywords: Metallic glasses Machine learning Combinatorial method Glass forming ability

ABSTRACT

Rational materials design out of vast compositional space is attractive yet challenging. The data-driven approach has shown promise in accelerating the development of advanced multicomponent alloys, such as metallic glasses. However, data-driven development of glass-forming alloys is limited by the sparse and biased datasets. In this study, we establish the high-throughput experimental database (HED), featuring an unprecedented quantity and diversity of experimental data. This database, encompassing 15,080 materials from 33 alloy systems synthesized and characterized under consistent conditions, provides a robust dataset for the training of machine learning model. The developed model is validated by both literature data and high-throughput experiments, and enables the creation of a catalogue of metallic glass forming alloy systems. The catalogue would serve as a practical reference for efficient design of glass-forming alloys systems.

1. Introduction

Since the discovery back in 1960, metallic glasses (MGs) have attracted enormous fundamental and technological interests [1]. The observation of glass formation in numerous alloy systems and even in pure metals [2,3], urges researchers to find the pivotal factors determining glass forming ability (GFA) of an alloy and MGs with desired properties. It is well known that a fast enough cooling rate is sufficient condition for producing MGs. However, the critical cooling rate, which is not readily measurable, can vary orders of magnitude from one alloy to another. For over six decades, numerous investigations have been carried out to obtain a comprehensive understanding of the factors that influence the ease of glass formation. Although these have been discussed from the perspectives of alloying effect, geometrical effect, configurational entropy, enthalpy of mixing, chemical bonding, and stabilization of liquid [4-9], the diverse constituent and the complex composition make the design of MGs notoriously challenging. Current design of MG-forming alloy systems remains mainly dependent on the empirical rules proposed by Inoue [10] and the search of deep eutectic composition within a phase diagram [11].

In order to accelerate the design and search of glass-forming alloys, data-driven approaches and machine learning (ML) have been recently

employed to construct the correlation of alloy compositions with GFA [12–16]. ML models with prediction accuracy better than 95 % have been claimed [15,17,18]. However, few successes of the ML approaches in developing new glass-forming alloys have been reported. One reason lies in the fact that most ML efforts in the field of MGs primarily rely on literature data accumulated through traditional trial-and-error methods [19]. These data were often collected under inconsistent preparation conditions, such as different cooling rates. In addition, the data often excludes the failures, leading to imbalanced data distributions with the successful samples dominating the datasets. Due to the limitation in high-quality data, a significant amount of ML research on MGs is devoted to identifying suitable physical parameters to improve model accuracy [13,18,20,21]. While certain thermodynamic parameters have been shown to be effective in specific alloy systems [11], they can only be determined after successful alloy synthesis. Furthermore, previously established physical parameters derived from weight-averaged elemental composition and properties may fail to accurately represent the characteristics of the alloy because many-body interactions are far more complex than the weighted average. In fact, the use of chemical composition as descriptors may leads to ML models that surpassed the ones using the calculated descriptors [15], because the variation range of these calculated quantities within an alloy system is significantly

^{*} Corresponding authors.

E-mail addresses: sunyitao@iphy.ac.cn (Y. Sun), yanhui.liu@iphy.ac.cn (Y. Liu).

[#] Equal contributions to this work

smaller than that caused by the change of constituent elements.

It is estimated that approximately 3000,000 compositions of MG remain to be discovered [22]. However, the number of reported MGs is limited to around 5000, with even fewer than 1000 being classified as bulk metallic glasses (BMGs), representing merely a small fraction of potential BMGs. In contrast to traditional material data collections that results in inconsistent data and data scarcity in glass formation, combinatorial fabrication paired with high-throughput characterizations not only enable rapid data collection of a large number of alloys under identical experimental conditions, but also overcome the imbalanced data distribution because both successful and unsuccessful samples can be obtained [23–25]. It is believed that these advantages benefit the training of more reliable ML models for the prediction of glass formation [12,26].

In this study, we fabricated combinatorial alloy libraries and employed X-ray diffraction (XRD) techniques to characterize the structure. These result in comprehensive high-throughput experimental database (HED). Our extensive characterizations encompassing approximately 15,000 alloys spanning 33 ternary systems, of which 51% are glass while 49% are crystals. The remarkable abundance of high-quality data acquired under consistent fabrication and characterization conditions are expected to enable the construction of more reliable ML models for glass formation. Due to the fact that the precise mechanisms of glass formation are not well understood yet, we focus on the prediction of glass-forming alloy systems (GASs), rather than the GFA of specific compositions. This allows the creation of a catalogue of GASs which can serves as a practical reference for the design and development of MGs of desired properties.

2. Results and discussion

It is well known that the quality and relevance of the training data is

paramount to the success of ML models and essentially determines the prediction accuracy of the trained model when algorithms and descriptors are given. In order to accumulate sufficient volume of consistent dataset, we collect experimental data by combinatorial synthesis paired with high-throughput characterizations. Specifically, we create, by employing magnetron co-sputtering deposition, combinatorial alloy libraries that cover a broad range of alloy composition [23,25,27]. The high effective cooling rate of sputtering deposition allows vitrification of alloys in a wide composition range, so that glass formation tendency within the alloy systems can be better revealed. The compositional spread of the library is unveiled by automated chemical analyses based on energy dispersive X-ray spectroscopy (EDX). We distinguish the GASs by characterizing the synthesized combinatorial alloy libraries through X-ray diffraction mapping [24]. We identify the glassy structure based on the width and symmetry of the first diffraction peak of the XRD pattern [24,28]. The analyses and characterizations results in binary information within the library, that is, glass versus crystal. The alloy systems that include glass are considered as GASs, while that only include crystals are considered as non-GASs. Typical GASs and non-GASs are given in Fig. 1a and b. For example, none of the alloys within the ternary Ag-Co-Cr system (Fig. 1a) form glass even the effective cooling rate is as high as 10^9 K/s [29]. In contrast, glass formation is achieved in a broad compositional range within the Co-Nb-Ir system (Fig. 1b).

We consider 21 elements that are commonly used as constituent elements for MGs. The elements include transition metals (Ti, V, Cr, Fe, Co, Ni, Cu, Zr, Nb, Ag, Ta, W, Ir, Pt, Au), rare earth elements (Y, Gd), alkaline-earth metals (Mg), metalloids (Si), and metals in the IIIB group (Al, Sn). We synthesized and characterized $\sim\!15,000$ alloys from 33 alloy systems, which cover all the 21 elements considered in this investigation (listed in Table S1). Analyses into the XRD patterns indicate that nearly half of the $\sim\!15,\!000$ alloys form glass under conditions of sputtering deposition (Fig. 1c). It is worth noting that the volume of our database is

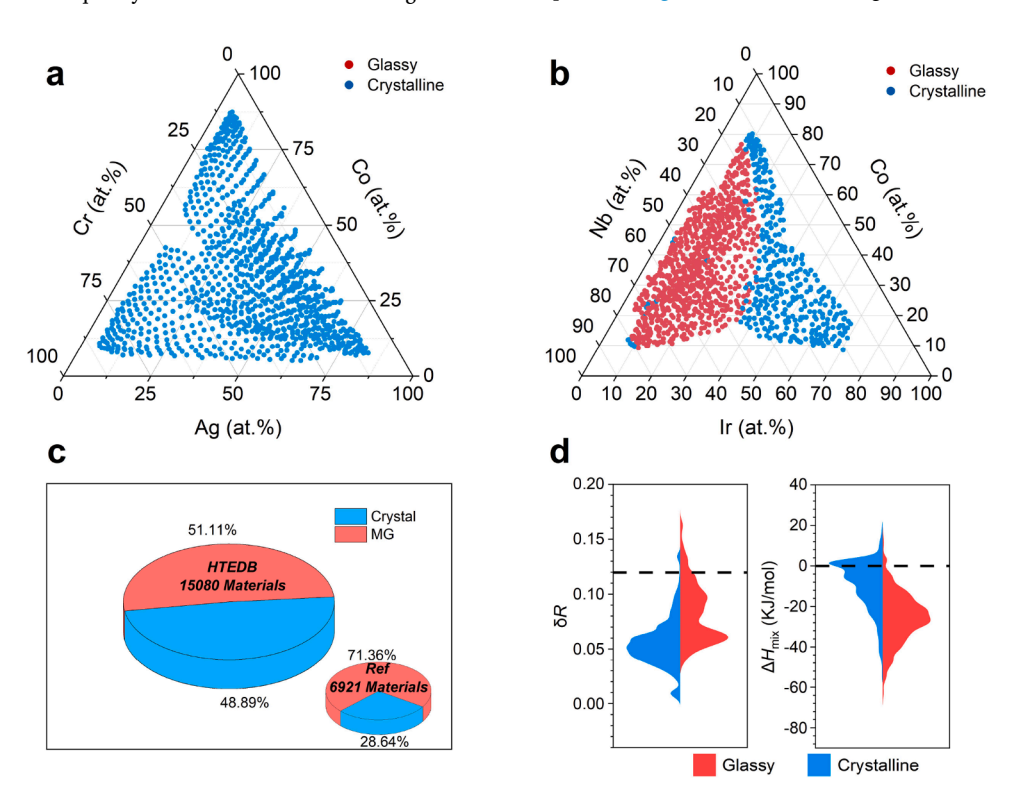


Fig. 1. Combinatorial method and high-throughput experimental database (HED). Structural information derived from X-ray diffraction pattern analysis of (a) Ag-Co-Cr and (b) Ir-Co-Nb thin film libraries, showing a distinct phase boundary between glassy and crystalline regions. (c) The HED comprises 15,080 materials, with amorphous and crystalline alloys accounting for 51.11 % and 48.89 %, respectively. The pie chart at the lower right shows the distribution of literature dataset. The 6921 materials are composed of 71.36 % amorphous materials and 28.64 % crystalline materials. (d) The distribution of glassy and crystalline alloys based on atomic radius mismatch and average mixing enthalpy. The black dashed line represents the empirical Inoue's rule, where atomic radius mismatch >12 % and mixing enthalpy <0 kJ/mol.

W. Xie et al. Materialia 39 (2025) 102375

more than two times larger than that accumulated from the literature reported over the past six decades [12]. The database, including both positive (glass formation) and negative (crystal formation) samples, is vast and comprehensive enough to train the ML model. In addition, the combinatorial fabrication and high-throughput characterization can readily provide new data on glass formation, so that the ML model can be iteratively optimized. According to the XRD characterizations, 27 out of the 33 alloy systems are GASs.

Because of its excellent classification performance [20,30,31], support vector machine (SVM) algorithm is chosen for model training. To optimize the hyperparameters, we employ a system-grouped cross-validation strategy (SGCV) to separate the database into multiple distinct groups based on alloy systems. This is different from the conventional partition method with which the entire dataset is split into the training and testing sets arbitrarily or using common k-fold cross-validation. Specifically, we divide the 33 systems into 10 equally-sized groups and ensure that each alloy within a given system is allocated to a single group. Nine of the ten groups are used to train the model, and the rest one is used to evaluate the accuracy of the trained model. The grouping, training, and evaluating is iterated ten times so that each group can serve as both the training dataset and testing dataset. The overall performance of the model is evaluated by the averaged accuracy over ten iterations. There are two advantages to group the experimental data with SGCV. Firstly, it ensures that the sample size is approximately equal from one group to another. This is in distinct contrast to previous report in which the sample sizes vary greatly. Secondly, it prevents data leakage, i.e. the repeated presence of alloy data from an identical alloy system in different groups. Therefore, the predictions of so-trained model can be considered as extrapolation instead of interpolation.

According to Inoue, the efforts to identify alloys of strong GFA should be made in the alloy systems that satisfy three empirical rules: (1) multicomponent systems consisting of three or more elements; (2) atomic size mismatches above 12 % among the main constituent elements; and (3) negative mixing enthalpy among the main constituent elements [32]. It is worth noting that the empirical rules were proposed for the design of alloy systems, rather the design of an alloy of specific composition. It is in the systems satisfying the rules that alloys of strong GFA can be possibly discovered. We analyzed the distribution of atomic size differences (δ_R) and weight-averaged mixing enthalpy (ΔH_{mix}) of the synthesized ~15,000 ternary alloys from the 33 alloy systems. Obvious differences in the distribution of glass-forming and crystal-forming alloys is revealed (Fig. 1d). For example, the distribution of δ_R shift towards larger values and the mixing enthalpy ΔH_{mix} is more negative for the glass-forming alloys, which is in excellent consistence with Inoue's empirical rules. We therefor take δ_R and ΔH_{mix} as the descriptors for the training of ML model that is for the prediction of GAS. In addition, a GAS is often characterized by the presence of eutectic points lying at relatively low temperature in the phase diagram [33], The underlying mechanism has been attributed to either stabilization of liquid phase [11] or the destabilization of crystalline mixture [33]. As a consequence, we incorporate the liquidus temperature reduction (ΔT) as an additional descriptor of our algorithm. Specifically, we calculate the concentration-weighted average of the constituent binary pairs' liquidus temperatures to extrapolate the liquidus temperature of the alloy, which is subsequently normalized by the mean liquidus temperature among the constituent elements [15]. We iterate that our focus is the prediction of GASs, not specific alloy compositions. To minimizing the influence of compositional deviations, we use the trained model to predict all glass-forming alloys within the binary, ternary, quaternary, and quinary systems constituted by the considered 21 elements.

We next train the model with the selected descriptors and the collected data by combinatorial syntheses and high-throughput characterizations. In order to improve generalization, we train the model iteratively with increasing size of dataset and evaluate the generalization of the model trained with N alloy systems by comparing the

predicted glass formation in N + 1 alloy system with experimental characterization on this N+1 system. More than 100 times iterations with random sequences of increasing number of alloy systems were performed to obtain statistically meaningful evaluation of the prediction accuracy. Fig. 2a displays the prediction accuracy, Pnext, of glass formation in the N + 1 alloy system as a function of the number of alloy systems used as training dataset. Evidently, with more alloy systems used for training, the prediction accuracy, Pnext, monotonically increases. Even with data only from three alloy systems, a P_{next} higher than 70 % can be obtained. When we take 32 alloy systems as training dataset, the prediction accuracy reaches a value of ~ 85 % (Fig. 2a). In addition, the standard deviation of accuracy, ΔP_{next} , decreases from 28 % to 18 % when the number of alloy systems used for training increases from N=3 to N=32 (Fig. 2b). The high prediction accuracy and low standard deviation of accuracy confirms that the three parameters (δ_R , ΔH_{mix} , ΔT) capture the essential characteristics of GASs. We notice that the prediction accuracy of the model improves if dataset from more alloy systems are used for training. However, the rate of improvement becomes slow when the number of training systems exceeds 30. For example, a logarithmical fit to P_{next} indicates that 1250 ternary alloy systems are required to reach a prediction accuracy of 95 % (see Fig. S1), which accounts for 94 % of the total possible ternary alloy systems (1330). This estimate implies that in addition to δ_R , ΔH_{mix} , and ΔT , other unknown parameter also plays a role in the predictability of the model. Considering the balance between accuracy and experimental feasibility, the final ML model is trained using 33 alloy systems (2.48 % of the 1330 ternary alloy systems), achieving a 10-fold SGCV accuracy of 85.46 %. Since machine learning models are more suitable for interpolation, the model's accuracy tends to be higher when predicting systems that are similar to the training systems, whereas it decreases when predicting systems that are entirely different. For instance, if the training data includes the Zr-Cu-Al system, the model will likely achieve higher accuracy in predicting systems with shared elements, such as Zr-Ni-Al, but lower accuracy for systems with no common elements, such as Mg-Cu-Y. Although the iteration curve in Fig. 2 represents the results of 100 random sequences, the presence of both similar and entirely different systems in the dataset inevitably leads to fluctuations in the iteration curve.

In addition to the model trained using HED, we trained another model by using literature dataset (LD) [12,34] and compared the prediction accuracy of the two models. The literature dataset are those from the alloy systems composed by the considered 21 elements which cover 94 alloy systems including many quaternary and even septenary alloy systems. We conducted a comprehensive cross-validation by comparing the prediction accuracy of GASs for four dataset combinations: (1) HED as both training and testing datasets (CV1), (2) HED as training dataset and LD as testing dataset (CV2), (3) LD as training dataset and HT data as testing dataset (CV3), and (4) LD as both training and testing datasets (CV4). In the context, the results of CV1 and CV4 represents the model's accuracy obtained through 10-fold SGCV using HED and LD. The models are subsequently employed to predict glass formation in LD space and HED space, respectively. It turns out that both models exhibit nearly identical accuracy of 82.20 % in predicting glass formation in LD space. However, in predicting glass formation in the HED space, the model trained with LD yields an obviously lower prediction accuracy of 78.23 % than that using the model trained using HED (85.46 %). The comparisons unambiguously demonstrate that the model train with HED outperforms that with LD. Although the LD encompass broader compositional range, the higher prediction accuracy of the model trained using HED underscore the essential role of large volume of consistent and balanced data in enhancing the generalization capability of the trained model. We believe that the generalization capability of the model arises from two key aspects. Firstly, although the number of systems included in HED is less than that of LD, the number of alloys within each system leads to a total sample size in HED that significantly exceeds that of LD. Secondly, many systems in the LD dataset are not W. Xie et al. Materialia 39 (2025) 102375

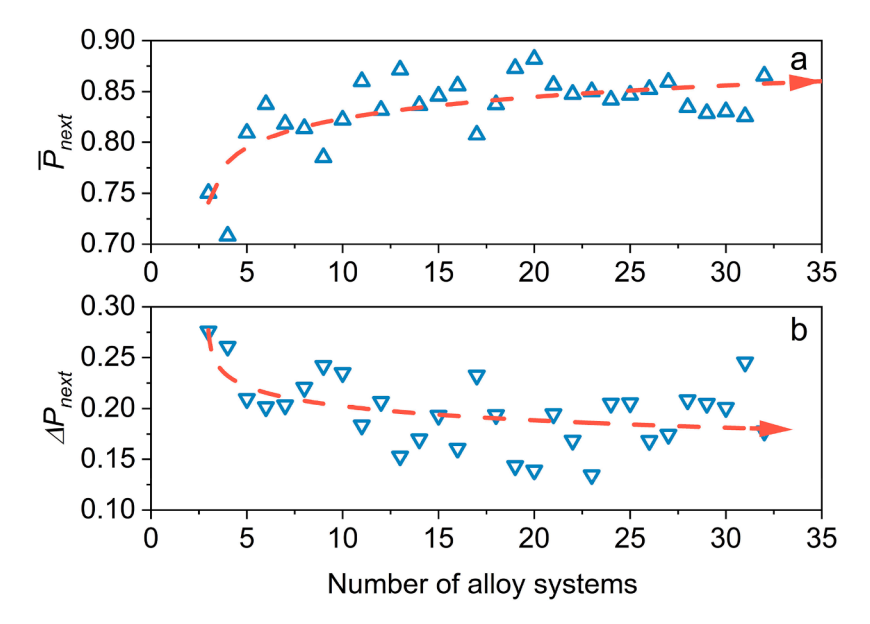


Fig. 2. Iterative improvement of the ML model. The average prediction accuracies (a) and corresponding standard deviations (b) for the next alloy system, using SVM models trained on varying numbers of alloy systems in the HED. Results are based on 100 independent random sequences of the 33 alloy systems, ensuring statistical validity. Adding more alloy systems to the training set significantly enhances prediction accuracy and reduces deviation.

entirely novel alloy systems; rather, they are variants of ternary systems, which likely exhibit a distribution in the feature parameter space similar to that of ternary systems.

We also computed the accuracy of the trained model using frequently adopted random 10-fold cross-validation. This yields an impressive accuracy of 94.60 %, which is at the same level as the accuracy reported in the literature [12,13,17,34,35]. However, we believe that this is an overestimated accuracy. The reason is that the random 10-fold cross-validation approach cannot avoid the data from the same alloy system to be present in both training and testing datasets even though simultaneous presence of alloys in both the training and testing sets is prevented [36–38]. Since the SGCV strategy effectively prevents data leakage, we take the accuracy of 85.46 % to reflect the generalization ability of our SVM model.

The well-trained ML model enables us to build a comprehensive category of GASs. Our SVM model predicts that 74 binary (35.25 % of 210) and 821 ternary (61.72 % of 1330) are GASs. Among them, 21 binary and 78 ternary alloy systems have been reported to be GAS.

The 21 elements that are considered in this study can form 210 binary and 1330 ternary alloy systems. We separate GASs from non-GASs by looking into the hyperplane created by the trained model in the feature space. Usually, the decision function (d_{alloy}), or the distance between a sample and this hyperplane, reflects the likelihood for a sample to be in the GAS category or not. We calculate the decision function for every composition within an alloy system and take the maximal values (P_{MG}) as the probability for the system being a GAS. Among the 1330 ternary alloy systems, 821 systems exhibit P_{MG} value greater than 0, while the $P_{\rm MG}$ values of the remaining systems are negative. We evaluate the accuracy of our ML model by comparing the P_{MG} values of predicted ternary GASs with the previously reported ternary GASs. Fig. 3a shows the distribution of P_{MG} for the 1330 ternary alloy systems. Two obvious peaks can be seen at $P_{\text{MG}}=-1$ and $P_{\text{MG}}=2$. The bimodal distribution $P_{\rm MG}$ indicates the remarkable accuracy of the hyperplane in differentiating crystalline and amorphous systems in the feature space. Meanwhile, one can see that P_{MG} of 94.87 % (74 out of 78) reported ternary GASs are located on the positive side with $P_{\rm MG}$ =3. It is noteworthy that our model predicts nearly all of previously known ternary GASs composed of the considered 21 elements. The only four (5.13 % of 78 known ternary GASs [39]) systems reported in literature that have not been successfully classified are Al-Cu-V, Cu-Nb-Ti,

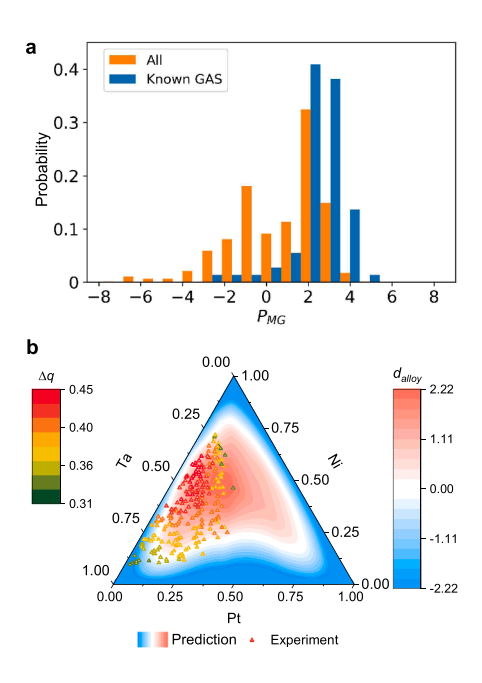


Fig. 3. Predictive performance of ML model. (a) Distribution of P_{MG} for 1330 ternary alloy systems (representing all possible combinations of the 21 elements in the HED) by the ML model (orange bars), compared with the distribution of reported GASs (blue bars). (b) Comparison of ML predictions (contour plot of the decision function d_{alloy}) with high-throughput experimental results (scatter plot with a colormap of Δq) for the Pt-Ni-Ta alloy system.

Cu-Nb-Sn, and Ag-Cu-Fe. Specifically, the Al-Cu-V and Cu-Nb-Ti alloys can only be fabricated via the melt-spinning technique, resulting in samples with remarkably small critical dimensions of only 0.02 mm [40, 41]. The Cu-Nb-Sn alloy has been obtained merely in the form of small-sized powder samples through the high-energy ball-milling technique [42]. The Ag-Cu-Fe alloys was synthesized using magnetron sputtering with a liquid nitrogen-cooled substrate [43], thus experiencing a significantly higher cooling rate compared to the room temperature magnetron sputtering employed in this study. These alloy

systems with poor GFA proves the robust capability of our model to accurately identify GAS.

According to the calculation, $P_{\rm MG}$ of previously unknown Pt-Ni-Ta alloy system is 2.219, a value far from the hyperplane. This suggests a high probability to obtain glass-forming alloys within the system. To confirm the prediction, we fabricate the combinatorial alloy libraries and perform chemical and structural characterization. As shown in Fig. 3b, glass formation can be observed in a broad compositional range. It is also interesting to note that the variation tendency of the full-width at half-maximum, Δq , of the first diffraction peak coincide with that of the value of decision function within the system. Since Δq is correlated with ease of glass formation of an alloy [24], the coincidence implies that d_{alloy} may be used as a measure of the glass formation once the GAS is predicted by the SVM model.

In addition to the binary and ternary alloy systems, considered 21 elements can form 5985 quaternary and 20,349 quinary systems. Among them, 28 quaternary and 19 quinary alloy systems have been reported to be GAS. Our SVM model predicts that out of the quaternary and quinary alloy systems, 76.69 % quaternary (4590 out of 5985) and 85.41 % quinary (17,380 out of 20,349) systems are GASs. Considering that 35.25 % binary (74 out of 210) and 61.72 % ternary (821 out of 1330) systems are GASs, one can conclude that the likelihood to form glass increases with the increased number of constituent elements in an alloy system. This is in consistence with the "confusion principle" [44]. In addition, the prediction indicates that only a tiny fraction of GASs have been developed. In particular, there are great potential to discover high-performance MGs in multicomponent alloy systems [22]. We catalogue the predicted GASs in supplementary online information (Table S1). The catalogue allows prompt identification of the relevant alloy systems which define the compositional space to be explored. Compared to the conventional trial-and-error development of metallic glasses, the comprehensive catalogue of GASs generated by our model would enable efficient target-oriented design of novel MGs. It should be noted that light elements, such as B, C, P, are not included the current study, despite their important role in glass formation. The exclusion is primarily due to the difficulties in controlling their sputter-deposition and accurately quantifying their concentrations using EDX. The uncertainty resulting from inaccurate quantification can lead to unreliable prediction. However, it is also important to note that attempts have been made to achieve high-throughput quantification of light elements by combining EDX with atom probe tomography (APT) [45-48]. These endeavors may pave the way for future studies on GAS-catalogue that cover a broader range of elements than those considered in the present work.

The categorization accuracy of the model is substantially higher than that of rule-guided human intuition. We take the reported GAS to testify the accuracy of rule-guided human intuition. The alloy systems are marked as GAS if they contain compositions with atomic radius differences greater than 12 % and average negative enthalpy of mixing as glass-forming alloy systems [10]. It turns out that the rule-guided human intuition only recognizes 33.33 % (7 out of 21) known binary and 53.85 % (42 out of 78) known ternary GASs. In contrast, the ML model we have developed is not only able to identify over 90 % of the known binary and ternary GASs but also predict all known quaternary and quinary GASs. While our SVM model is built upon previously established empirical rules, it significantly outperforms human intuition guided by these rules. This originates from the utilization of balanced training dataset and the intrinsic capability of SVM model to deal with complex, non-linear variables.

3. Conclusion

In summary, we employ high-throughput experimental preparation and characterization to obtain a high-quality database known as HED, subsequently training a machine learning model to predict glass-forming alloy systems. The HED encompasses 33 alloy systems composed of 21

distinct elements, totaling 15,080 materials, all of which share uniform preparation conditions and exhibit balanced distribution. Utilizing the well-trained ML model, we present a comprehensive catalogue comprising 74 binary, 821 ternary, 4590 quaternary, and 17,380 quinary glass-forming alloy systems. With this catalogue, one can swiftly identify the elemental combinations for development of MG with desired properties.

4. Methods

4.1. ML algorithms

The machine learning (ML) algorithms were implemented using Python and the Scikit-learn (v1.2.0) library. A Support Vector Machine (SVM) model with an RBF kernel was trained, with the hyperparameters C and gamma optimized to 10 and 0.01, respectively, using a 10-fold system-grouped cross-validation method. Default values were used for all other parameters.

4.2. Model iteration

Predictions for the N+1 unknown alloy system were made using an optimized ML model trained on the first N alloy systems, following a randomized order, for N ranging from 3 to 32. To reduce the impact of randomness and better capture the true trend as the dataset grows, the prediction process was repeated 100 times with random sequences of alloy systems.

4.3. Library fabrication

Combinatorial thin-film libraries were fabricated via magnetron cosputtering deposition (SKY Technology Development Co., Ltd., Chinese Academy of Sciences, TRP450) onto 100-mm-diameter single-side-polished Si wafers, using three pure metal sputtering targets with a purity of over 99.95 %. The base pressure was lower than 10^{-4} Pa, and a working pressure of 1.0 Pa was maintained by flowing ultrahigh purity argon during spuettering. The thickness of the deposited films is about 1 μm with a deposition rate of $\sim\!100$ Å/min. For each alloy system, 3–4 experiments with adjusted sputtering power were conducted to cover the majority of the compositonal space.

4.4. Materials characterization

Compositions and structures of the combinatorial libraries were automatically characterized by EDX attached to a Phenom scanning electron microscope and a Malvern PANalytical Empyrean X-ray diffractometer with a Cu K α radiation source, respectively. XRD patterns for each alloy were processed using programs developed in ref [24] to reveal the distribution of amorphous and crystalline phases.

Data availability

The authors declare that the data supporting the findings of this study are included within the paper and available from the corresponding author on reasonable request. Both experimental and predicted data will be made available at https://cmpdc.iphy.ac.cn/mgdb/.

CRediT authorship contribution statement

Weijie Xie: Writing – review & editing, Writing – original draft, Validation, Methodology, Investigation, Formal analysis, Data curation. Mingxing Li: Funding acquisition, Formal analysis, Data curation. Yitao Sun: Methodology, Investigation, Funding acquisition, Formal analysis, Data curation. Chao Wang: Resources, Methodology, Investigation, Data curation. Liwei Hu: Data curation. Yanhui Liu: Writing – review & editing, Writing – original draft, Supervision, Methodology, Funding

acquisition, Formal analysis, Conceptualization.

Declaration of competing interest

The authors declare that they have no known competing financial interests or personal relationships that could have appeared to influence the work reported in this paper.

Acknowledgements

We thank J.S. Cao and F. Yang for experimental assistance. The work was financially supported by the National Natural Science Foundation of China (grant nos. 52331007, 52192602, T2222028, 52101206) and the National Key Research and Development Program of China (grant no. 2021YFA0718703).

Supplementary materials

Supplementary material associated with this article can be found, in the online version, at doi:10.1016/j.mtla.2025.102375.

References

- [1] W. Klement, R.H. Willens, P. Duwez, Non-crystalline Structure in Solidified Gold–Silicon Alloys, Nature 187 (1960) 869–870, https://doi.org/10.1038/ 187869b0
- [2] W.H. Wang, C. Dong, C.H. Shek, Bulk metallic glasses, Mate. Sci. Eng.: R: Rep. 44 (2004) 45–89, https://doi.org/10.1016/j.mser.2004.03.001.
- [3] L. Zhong, J. Wang, H. Sheng, Z. Zhang, S.X. Mao, Formation of monatomic metallic glasses through ultrafast liquid quenching, Nature 512 (2014) 177–180, https:// doi.org/10.1038/nature13617.
- [4] Y.-C. Hu, H. Tanaka, Physical origin of glass formation from multicomponent systems, Sci. Adv. 6 (2020) eabd2928.
- [5] Y.-C. Hu, J. Schroers, M.D. Shattuck, C.S. O'Hern, Tuning the glass-forming ability of metallic glasses through energetic frustration, Phys. Rev. Mater. 3 (2019), https://doi.org/10.1103/PhysRevMaterials.3.085602.
- [6] Z.W. Wu, M.Z. Li, W.H. Wang, K.X. Liu, Hidden topological order and its correlation with glass-forming ability in metallic glasses, Nat. Commun. 6 (2015) 6035. https://doi.org/10.1038/ncomms7035.
- [7] Y.F. Ye, C.T. Liu, Y. Yang, A geometric model for intrinsic residual strain and phase stability in high entropy alloys, Acta Mater. 94 (2015) 152–161, https://doi.org/ 10.1016/j.actamat.2015.04.051.
- [8] E. Perim, et al., Spectral descriptors for bulk metallic glasses based on the thermodynamics of competing crystalline phases, Nat. Commun. 7 (2016) 12315, https://doi.org/10.1038/ncomms12315.
- [9] J. Russo, F. Romano, H. Tanaka, Glass forming ability in systems with competing orderings, Phys. Rev. X 8 (2018) 021040.
- [10] A. Takeuchi, A. Inoue, Classification of bulk metallic glasses by atomic size difference, heat of mixing and period of constituent elements and its application to characterization of the main alloying element, Mater. Trans. 46 (2005) 2817–2829, https://doi.org/10.2320/matertrans.46.2817.
- [11] D.M. Turnbull, Under what conditions can a glass be formed, Contemp. Phys. 10 (1969) 473–488.
- [12] Z.Q. Zhou, et al., Rational design of chemically complex metallic glasses by hybrid modeling guided machine learning, NPJ Comput. Mater. 7 (2021), https://doi.org/ 10.1038/s41524-021-00607-4.
- [13] J. Xiong, S.-Q. Shi, T.-Y. Zhang, A machine-learning approach to predicting and understanding the properties of amorphous metallic alloys, Mater. Des. 187 (2020) 108378, https://doi.org/10.1016/j.matdes.2019.108378.
- [14] L. Ward, et al., A machine learning approach for engineering bulk metallic glass alloys, Acta Mater. 159 (2018) 102–111, https://doi.org/10.1016/j. actamat.2018.08.002.
- [15] G. Liu, et al., Machine learning versus human learning in predicting glass-forming ability of metallic glasses, Acta Mater. (2022) 118497, https://doi.org/10.1016/j. actamat.2022.118497.
- [16] G. Liu, S. Sohn, C.S. O'Hern, A.C. Gilbert, J. Schroers, Effective subgrouping enhances machine learning prediction in complex materials science phenomena: inoue's subgrouping in discovering bulk metallic glasses, Acta Mater. 265 (2024) 119590, https://doi.org/10.1016/j.actamat.2023.119590.
- [17] S Feng, et al., A general and transferable deep learning framework for predicting phase formation in materials, NPJ Comput. Mater. 7 (2021), https://doi.org/ 10.1038/s41524-020-00488-z.
- [18] D. You, et al., Electrical resistivity as a descriptor for classification of amorphous versus crystalline phases of alloys, Acta Mater. 231 (2022) 117861, https://doi. org/10.1016/j.actamat.2022.117861.

- [19] Y. Kawazoe, J.-Z. Yu, A.-P. Tsai, T. Masumoto, Nonequilibrium phase diagrams of ternary amorphous alloys (1997).
- [20] Y.T. Sun, H.Y. Bai, M.Z. Li, W.H. Wang, Machine learning approach for prediction and understanding of glass-forming ability, J. Phys. Chem. Lett. 8 (2017) 3434–3439, https://doi.org/10.1021/acs.jpclett.7b01046.
- [21] B. Deng, Y. Zhang, Critical feature space for predicting the glass forming ability of metallic alloys revealed by machine learning, Chem. Phys. (2020) 538, https://doi. org/10.1016/j.chemphys.2020.110898.
- [22] Y. Li, S. Zhao, Y. Liu, P. Gong, J. Schroers, How many bulk metallic glasses are there? ACS Comb. Sci. 19 (2017) 687–693, https://doi.org/10.1021/ acscnmbsri.7b00048
- [23] M.-X. Li, et al., High-temperature bulk metallic glasses developed by combinatorial methods, Nature 569 (2019) 99–103, https://doi.org/10.1038/s41563-021-01129-6
- [24] M.-X Li, et al., Data-driven discovery of a universal indicator for metallic glass forming ability, Nat. Mater. (2021), https://doi.org/10.1038/s41563-021-01129-
- [25] F. Ren, et al., Accelerated discovery of metallic glasses through iteration of machine learning and high-throughput experiments, Sci. Adv. 4 (2018) eaaq1566.
- [26] Y. Yao, T. Sullivan, F. Yan, J. Gong, L. Li, Balancing data for generalizable machine learning to predict glass-forming ability of ternary alloys, Scr. Mater. 209 (2022) 114366, https://doi.org/10.1016/j.scriptamat.2021.114366.
- [27] S Ding, et al., Combinatorial development of bulk metallic glasses, Nat. Mater. 13 (2014) 494–500, https://doi.org/10.1038/nmat3939.
- [28] A.M. Molodets, A.A. Golyshev, Structural transformations of amorphous carbon (Glassy Carbon) at high shock pressures, J. Exp. Theor. Phys. 126 (2018) 772–778, https://doi.org/10.1134/S1063776118060079.
- [29] Y.H. Liu, T. Fujita, D.P.B. Aji, M. Matsuura, M.W. Chen, Structural origins of Johari-Goldstein relaxation in a metallic glass, Nat. Commun. 5 (2014) 3238, https://doi.org/10.1038/ncomms4238.
- [30] C. Cortes, V. Vapnik, Support-vector networks, Mach. Learn. 20 (1995) 273–297, https://doi.org/10.1007/BF00994018.
- [31] R.G. Brereton, G.R. Lloyd, Support Vector Machines for classification and regression, Analyst 135 (2010) 230–267, https://doi.org/10.1039/B918972F.
- [32] A. Inoue, Stabilization of metallic supercooled liquid and bulk amorphous alloys, Acta Mater. 48 (2000) 279–306, https://doi.org/10.1016/S1359-6454(99)00300-6.
- [33] H.S. Chen, H.J. Leamy, C.E. Miller, Preparation of glassy metals, Annu Rev. Mater. Res. 10 (1980) 363–391, https://doi.org/10.1146/annurev.ms.10.080180.002051.
- [34] R.M. Forrest, A.L. Greer, Machine-learning improves understanding of glass formation in metallic systems, Digit. Discov. 1 (2022) 476–489, https://doi.org/ 10.1039/D2DD00026A.
- [35] Z. Zhou, et al., Machine learning guided appraisal and exploration of phase design for high entropy alloys, NPJ Comput. Mater. 5 (2019), https://doi.org/10.1038/ s41524-019-0265-1.
- [36] A. Rabinowicz, S. Rosset, Cross-Validation for Correlated Data, J. Am. Stat. Assoc. 117 (2019) 718–731.
- [37] J. Wieczorek, C. Guerin, T. McMahon, K-fold cross-validation for complex sample surveys, Stat. (2022) 11.
- [38] A. Vabalas, E. Gowen, E. Poliakoff, A.J. Casson, Machine learning algorithm validation with a limited sample size, PLoS One (2019) 14.
- [39] Y. Kawazoe, et al., Nonequilibrium phase diagrams of termary amorphous alloys, in: LB: New Series Group III 37, Condensed, Springer, 1996, pp. 1–295.
- [40] A.-P. Tsai, A. Inoue, T. Masumoto, Ductile Al-Cu-V amorphous alloys without metalloid, Metall. Trans. A 19 (1988) 391–393, https://doi.org/10.1007/ BF02652554.
- [41] A. Inoue, C. Suryanarayana, T. Masumoto, Microstructure and superconductivity in annealed Cu-Nb-(Ti, Zr, Hf) ternary amorphous alloys obtained by liquid quenching, J. Mater. Sci. 16 (1981) 1391–1401, https://doi.org/10.1007/ BF01033856.
- [42] A. Inoue, H.M. Kimura, K. Matsuki, T. Masumoto, Preparation of new amorphous Cu-Nb-Sn alloys by mechanical alloying of elemental copper, niobium and tin powders, J. Mater. Sci. Lett. 6 (1987) 979–981, https://doi.org/10.1007/ BF01729890.
- [43] K. Sumiyama, K. Nishi, M. Shiga, M. Sakurai, K. Suzuki, The amorphous structure of immiscible Fe-Cu-Ag alloys, J. Non. Cryst. Solids 150 (1992) 391–395, https://doi.org/10.1016/0022-3093(92)90159-H.
- [44] A.L. Greer, Confusion by design, Nature 366 (1993) 303–304, https://doi.org/ 10.1038/366303a0.
- [45] S. Evertz, et al., Boron concentration induced Co-Ta-B composite formation observed in the transition from metallic to covalent glasses, Condens. Matter. 5 (2020).
- [46] V. Schnabel, et al., Revealing the relationships between chemistry, topology and stiffness of ultrastrong Co-based metallic glass thin films: a combinatorial approach, Acta Mater. 107 (2016) 213–219, https://doi.org/10.1016/j. actamat.2016.01.060.
- [47] P. Kontis, et al., Nano-laminated thin film metallic glass design for outstanding mechanical properties, Scr. Mater. 155 (2018) 73–77, https://doi.org/10.1016/j. scriptamat.2018.06.015.
- [48] V. Schnabel, et al., Electronic hybridisation implications for the damage-tolerance of thin film metallic glasses, Sci. Rep. 6 (2016) 36556, https://doi.org/10.1038/ srep36556.